·Article·
Advances in Polar Science
doi: 10.3724/SP.J.1085.2013.00098
June 2013 Vol. 24 No. 2: 98-105

Modeling Arctic Intermediate Water: The effects of Neptune parameterization and horizontal resolution

LI Xiang[1,2*], SU Jie[1,2], WANG Zeliang[3] & ZHAO Jinping[1,2]

[1] Key Laboratory of Physical Oceanography, Ministry of Education, Qingdao 266003, China;
[2] College of Physical and Environmental Oceanography, Ocean University of China, Qingdao 266100, China;
[3] Bedford Institute of Oceanography, Department of Fisheries & Oceans, NS B2Y 4A2, Canada

Received 27 February 2013; accepted 15 May 2013

Abstract Arctic Intermediate Water (AIW), advected from the North Atlantic Ocean, has a potential influence on climate in the Arctic region, but is poorly simulated in coarse resolution models. In this study, a coupled ice-ocean model is used to investigate features of AIW by conducting two sensitivity experiments based on Neptune parameterization and horizontal resolution. The results show that both experiments improve the modeling of temperature profiles in the western Eurasian Basin, mainly as a result of more realistic volume and heat transport through the Fram Strait. Topographical flows are well reproduced using Neptune parameterization or a finer horizontal resolution. In the eddy-permitting model with relatively higher resolution, the velocity field is more realistic than in the Neptune parameterization model, and complex inflow and outflow belts of barotropic structure are well reproduced. The findings of this study suggest that increased model resolution, as provided by an eddy-resolving model, is needed to reproduce realistic circulation and thermohaline structure in the Arctic, since the Rossby radius of deformation is only several kilometers in the Arctic Ocean. This paper focuses on the external heat input rather than internal mixing process, and obtains a conclusion that the heat input from the Fram Strait is a main factor to reproduce AIW in the Eurasian Basin successfully, at least for the western part.

Keywords **Arctic modeling, Arctic Intermediate Water, Neptune parameterization, horizontal resolution**

Citation: Li X, Su J, Wang Z L, et al. Modeling Arctic Intermediate Water: The effects of Neptune parameterization and horizontal resolution. Adv Polar Sci, 2013, 24: 98-105, doi: 10.3724/SP.J.1085.2013.00098

1 Introduction

The Arctic Ocean is the most active region under the global warming scenarios in last few decades, and changes in the Arctic Ocean can be considered as a good indicator of global climate change according to IPCC AR4 (the Fourth Assessment Report of the Intergovernmental Panel on Climate Change)[1]. The Arctic Ocean has undergone many changes including a reduction in sea ice extent[2], and retreat of the cold halocline followed by a partial recovery[3-4]. Arctic Intermediate Water (AIW), usually known as the Atlantic Water Layer in the Arctic Ocean, lies at a depth of 150–1 000 m throughout the Arctic Ocean, and is characterized by relatively high temperatures of above 0℃[5]. This relatively warm water mass comes from the Nordic Seas with huge heat content and sinks to intermediate depths in the Arctic Basin. It is isolated by a strong halocline i.e. pycnocline, so the upward heat flux is restricted to ~2–4 $W \cdot m^{-2}$[3,6]. However, AIW does have an effect on sea ice and may influence surface sea ice distribution[5,7]. If the large amount of heat contained in AIW was convected up to the surface, there would be no sea ice in the Arctic Ocean, even in winter[8].

Atlantic Water enters the Arctic Ocean by two pathways. The main branch, the Fram Strait Branch (FSB), passes through the Fram Strait, which is the only deep connection between the Arctic Ocean and the Atlantic Ocean. The second branch, the Barents Sea Branch (BSB), passes through the Barents Sea Opening[9-11] (Figure 1). The BSB undergoes significant diffusion and convection processes in the shallow shelf Barents Sea, and most of the heat content

* Corresponding author (email: lixiangqd@126.com)

is lost before entering the Eurasian Basin through the St. Anna Trough[12]. This colder water mass lies below the FSB because it has a higher density. Atlantic Water moves cyclonically at the intermediate depth along the shelf slope around the entire Arctic Basin, forming the Arctic Circumpolar Boundary Current (ACBC)[10,13].

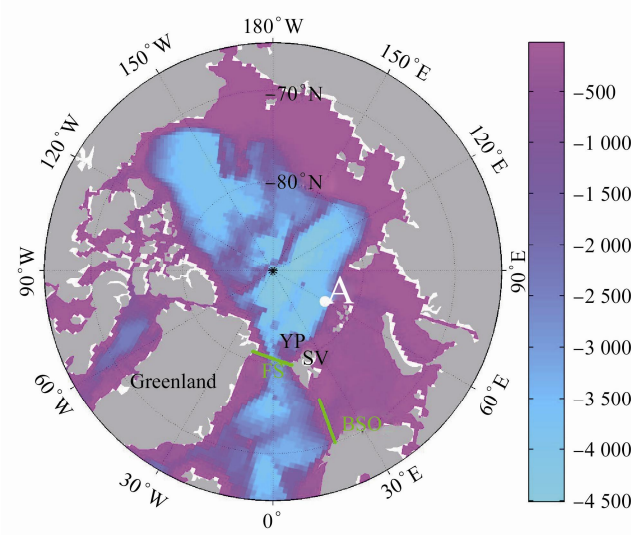

Figure 1 Bathymetry (m) of the Arctic Ocean in the ORCA1 grid area. The white dot is the location of station A. Green lines represent the Fram Strait (FS) and Barents Sea Opening (BSO). YP is the Yermak Plateau, and SV is the Svalbard.

Due to a relative lack of *in situ* observations in polar regions, numerical models are important tools for investigating changes in the Arctic. The Arctic Ocean Model Inter-comparison Project (AOMIP), established in 2001 by scientists from eight countries, aims to compare performances of the Arctic Ocean models and reduce scientific uncertainties[14-15]. At the start of the project, the modeled circulation at the intermediate depth did not reflect the traditional understanding of the flow pattern derived from sparse observational data[14]. Half of the models reproduced a cyclonic circulation, while the other half showed an anticyclonic circulation. Many improvements have been made to Arctic Ocean modeling over recent years, including the incorporation of potential vorticity (PV) flux[16] and Neptune effect parameterization[17-19]. The Neptune effect, first described by Holloway[17] and developed by Polyakov[19], has been included in models to generate a stable cyclonic circulation[20-21]. Neptune parameterization adds an explicit term in momentum equations as an entropic forcing so the topography provides a driving force as a result of eddy-topography interaction. It has been reported that ocean circulation is more realistic with Neptune parameterization in many regions throughout the world, according to data from ocean current meters[22]. However, the water properties have been poorly reproduced in AOMIP models[15]. The core temperature of the Atlantic Water is either too high or too low, or the depth is incorrect, although some models do generate a realistic circulation. There have been few studies published on the simulation of AIW and researchers have encountered various problems in modeling this water mass (personal communications at the AOMIP 2011 workshop). In this paper, we use a coupled ice-ocean model based on NEMO (Nucleus for European Modeling of the Ocean) to study Atlantic Water in the Eurasian Basin. Two sensitivity experiments were conducted, one using Neptune parameterization, and the other using a model with a high horizontal resolution, and the outputs were compared with a baseline run. A detailed description of the models will be presented next, and the problems of modeled AIW in the baseline run will be discussed. Then the improvements obtained by the Neptune run and high resolution run will be illustrated. Finally, remaining deficiencies in the two sensitivity experiments and some possible solutions will be discussed at the end of this paper.

2 Model description

The model used in this study is a coupled ocean-ice model based on NEMO 2.3[23], and includes an ocean general circulation model OPA (Ocean PArallelise)[24] and a simple ice model LIM (Louvain-la-Neuve Sea Ice Model) version 2[25]. The model domain is global and the two horizontal grids used, ORCA1 and ORCA025, are from the National Oceanography Centre, Southampton, UK. ORCA1 is a tri-polar nominal 1-degree grid (35–60 km in the Arctic) with finer resolution at equator and the Arctic. ORCA025 is similar to ORCA1 with the same position of three poles but a 0.25-degree grid (6–18 km in the Arctic). More details about ORCA grids can be found on the website: http://www.noc.soton.ac.uk/nemo/. For ORCA1, the vertical coordinate used is a z-level 46-layer grid and for ORCA025, the vertical coordinate is a z-level 50-layer grid (finer resolution near surface). The thickness of layers increases from the surface to the bottom (6 m and 1 m at the surface for the ORCA1 46-layer and ORCA025 50-layer grids, respectively, increasing with depth to 40 m for both ORCA1 and ORCA025 at 220 m). Li et al.[26] used a 76-layer grid and obtained results similar to those obtained using a 46-layer grid (ORCA1, as used in this study). They suggested the impact of the vertical resolution on AIW simulation can be omitted.

Surface forcing is obtained from the Ocean Model Inter-comparison Project (OMIP) version 3, based on ERA-40. The forcing incorporated daily climatology including 2 m air temperature, wind stress, cloud fraction, and relative humidity. No restoring to sea surface temperature (SST) is applied, but sea surface salinity (SSS) is restored to the climatology on a 15-day time scale.

The model starts in January with the initialization of climatological temperature and salinity from Polar Hydrographic Climatology (PHC) 2.1[27]. Where the SST is below 0℃, sea ice is initialized by a uniform thickness of 3 m and 1 m for the Northern and Southern Hemispheres, respectively, and snow is initialized by 0.5 m and 0.1 m in the Northern and Southern Hemispheres, respectively.

The vertical diffusivity and viscosity are computed from a 1.5-order turbulent closure scheme (turbulent kinetic energy, TKE). Isopycnal diffusion and eddy-induced tracer advection are applied according to GM90 (Gent and McWilliams[28]) with a diffusivity depending on the grid area, as recommended by Hunke et al.[29]. Eddy-induced advection is set to zero for the model using the ORCA025 grid. The time step is 3 600 s for the model using the ORCA1 grid and 1 200 s for the model using the ORCA025 grid, and the ice module is called every five steps. The models are run for 10 a driven by the OMIP forcing. Results for the early years are considered as spin-up time and the results of the last year are used for analysis in this paper. The viscosity and diffusivity differ between ORCA1 and ORCA025 due to different resolution.

There are three runs in total. The model grids and other details are presented in Table 1. Run A is the baseline run as described above, run B incorporates Neptune parameterization, and the vertical grid in run C has a higher horizontal resolution of 0.25 degree compared with 1 degree used for run A and run B. In this study, we focus on the impact of Neptune parameterization and the potential effect resulting from the increased horizontal resolution.

Table 1 Details of the model runs in this study

	Baseline (run A)	Neptune (run B)	025 run (run C)
Horizontal grid	ORCA1	ORCA1	ORCA025
Vertical levels	46	46	50
Initial T & S (interpolated into each grid)	PHC2.1	PHC2.1	PHC2.1
Surface forcing (interpolated into each grid)	OMIP v3	OMIP v3	OMIP v3
Neptune effect	No	Yes	No

3 Temperature profile

Li et al.[26] discussed the problem involved in modeling AIW in the Eurasian Basin. The most unsatisfactory results obtained from modeling of AIW were at the slope of the Eurasian Basin. In that paper, the temperature evolution in a time-depth plot at a location on the slope (station A, shown in Figure 1) was presented. Heat content was gradually lost during a 10-year model run and the model output showed excessive vertical mixing, caused by isopycnal diffusion, at a scale 100 times larger than estimated from observations in the Eurasian Basin. The problem was not solved by simply suppressing this parameterization, which implied that is was complex and caused by many factors. In this study, we focused on the sensitivity of heat input from the Atlantic Ocean rather than the mixing parameterization in the Arctic Ocean. The model we used was similar to that used by Li et al.[26], and detailed information on the model and model performances can be found in that paper.

Figure 2 shows temperature profiles from three runs at station A (Figure 1), the same station used by Li et al.[26]. After being driven by climatological forcing for 10 years, the baseline run A driftes from PHC. The Atlantic Water Core Temperature (AWCT), defined as the temperature maximum below halocline, is nearly 1℃ below that obtained from PHC and the depth of the AWCT is biased by about 200 m. In other words, nearly half of the heat content of AIW referring to 0℃ is lost in this 10-year climatological run. However, below 800 m, the temperature in the baseline run is higher than that in PHC. This may partly be a consequence of excessive vertical mixing caused by the GM90 parameterization[26]. This problem exists in the whole Eurasian Basin, especially along the slope, and we selected this station because it is significant in the region.

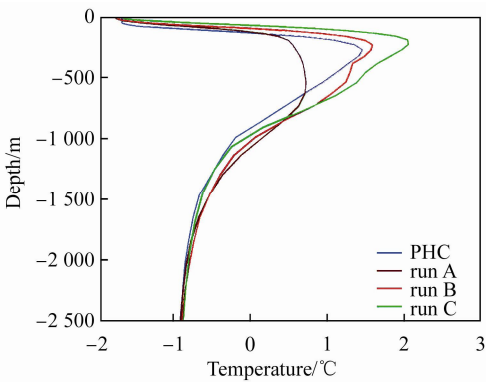

Figure 2 The annual mean temperature profiles at station A for the 10th year of the model run.

The simulated AWCT is significantly improved in run B using Neptune parameterization. The AWCT and its depth are well represented, although the Atlantic Water Layer is slightly thicker. The simulated AWCT in the higher horizontal resolution run C is 0.6℃ higher than that in PHC, but the depth agrees well with the PHC. Therefore, at this station, run B and run C can reasonably reproduce the vertical distribution of temperature of AIW.

4 Circulation

It has previously been reported that Neptune parameterization can improve the simulation of the ACBC[15,17-19], and this is confirmed in this study (Figure 3). The ACBC is not quite clear in run A (Figure 3a), especially in the Canada Basin. In run B, a stable cyclonic circulation can be reproduced, which was inferred from lots of thermohaline observations[9].

Even without Neptune parameterization, run C with a higher horizontal resolution reproduces a stable and more energetic cyclonic circulation at the intermediate depth (Figure 3c), indicating that the ACBC is possibly a topography-steered flow. Finer resolution topography as used in run C can better represents realistic topography with stronger water depth gradients at the shelf break, which is an important factor in Neptune parameterization, resulting

in a good representation of the ACBC. The interaction between eddies and topography can also play a significant role in this process, and this is achieved using the high-resolution eddy-permitting model. Neptune parameterization improved the model with a coarse resolution although the Atlantic Water inflow is underestimated, as discussed in the following section.

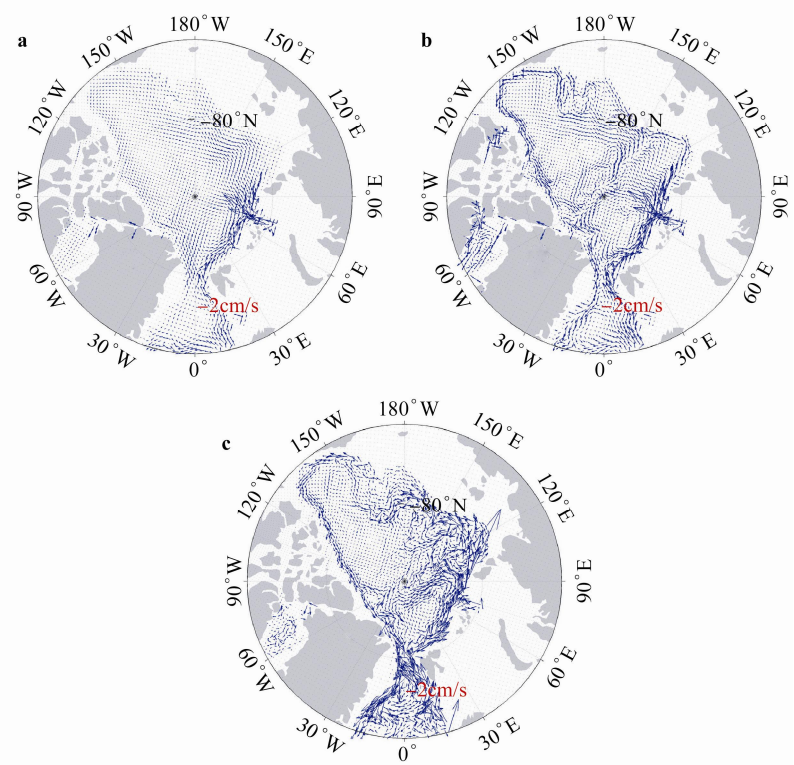

Figure 3 Annual mean circulation at 452 m for the 10th year of the three model runs: baseline run (**a**), Neptune parameterization run (**b**), and high horizontal resolution run (**c**).

Topostrophy has been used as a method to evaluate modeled ocean circulations[19,29-30]. It is usually defined as:

$$\tau = f \times V \cdot \nabla D$$

where f is the vertical Coriolis factor, V is the velocity vector of the model output, and D is the total depth. Positive topostrophy means flow is with shallower water to the right (cyclonic) in the Northern Hemisphere and with shallower water to the left (anticyclonic) in the Southern Hemisphere. Therefore, the direction of circulation can be readily determined by calculating topostrophy, which is especially useful for assessing flow around the basin margin.

Run B and run C accurately reproduce the topography-steered flow in the Greenland—Iceland—Norwegian (GIN) Seas and the Arctic Ocean (Figure 4b and 4c). Main improvements compared with the baseline run A (Figure 4a) include the identification of the West Spitsbergen Current (WSC), the East Greenland Current (EGC), the ACBC along the Canada Basin margin, and the re-circulation at the Lomonosov Ridge. The WSC is the main heat source for AIW. It carries warm and salty Atlantic Water into the Arctic Ocean through the Fram Strait. Once the Atlantic Water enters the Arctic Ocean, it sinks under the halocline then gradually loses heat by diffusion. The findings of this study suggest that the probable reason for the failure to reproduce AIW in run A is the lack of heat input from the Atlantic Ocean.

5 Transport of the Atlantic Water inflow

Atlantic Water enters the Arctic Ocean by two pathways that split in the Norwegian Sea. We set two sections (Figure 1) close to areas with available *in situ* observations to examine the heat transport from the Atlantic Ocean. The Fram Strait section (FS) is an x-direction model grid section in almost the same position as moorings studied by Schauer et al.[32]. The Barents Sea Opening section (BSO) is along the 20 degree meridian east as described by Skagseth et al.[33]. Note that for analysis, the model outputs are interpolated onto the sections using bilinear interpolation.

Observations were from different years and seasons and the transport through these major sections demonstrated significant interannual variability. The Fram Strait is the main pathway for warm Atlantic Water moving into the Arctic. Its volume transport is ~5 times larger than that of the BSO (Table 2) but the heat transport through these two segments is similar because the temperature of the inflow is higher at the BSO, which lies closer to the Atlantic Water

source. The BSB follows a long and meandering path before entering the Eurasian Basin in the shallow Barents Sea, a shelf sea with water depth of less than 500 m, usually free of ice even in winter, making it an area of energetic air—sea exchange. Most of the heat content in the BSB is lost to the surface and the atmosphere. Wang et al.[12] estimated that 89% of heat in the BSB was lost before entering the Eurasian Basin.

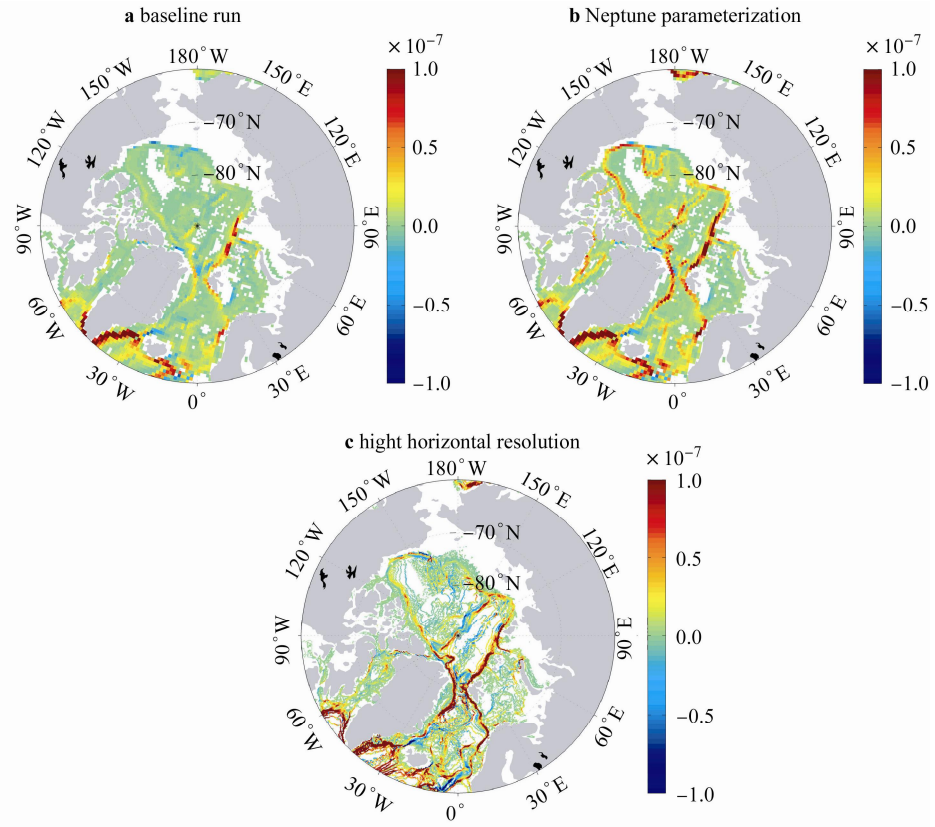

Figure 4 Annual mean depth-integrated topostrophy between 150–950 m for the 10th year of the three model runs.

Table 2 Annual mean volume and heat transport inflow (northward) through the Fram Strait and Barents Sea Opening into the Arctic Ocean

	Observed	Run A	Run B	Run C
FS volume (Sv)	9–10[1]	1.8	2.7	3.9
	12[2]			
BSO volume (Sv)	1.8[3]	4.6	3.6	1.9
	2.0[4]			
FS+BSO volume (Sv)		6.4	6.3	5.8
FS heat (TW)	32–55[1]	21	39	48
BSO heat (TW)	48[3]	105	87	60

Notes: [1]Observations at the FS are mooring data from Schauer et al.[32] for 1997–2000; [2]updated data from Schauer et al.[34] for 1997–2006; [3]Fluxes at the BSO are mooring data from Skagseth et al.[33] for 1997–2007; [4]Smedsrud et al.[35] for 1997–2007. All data are annual mean values.

Table 2 shows that all three model runs misrepresent the distribution of volume transport through the FS and the BSO as determined from observations. In the output from run A, less than 30% (1.8 of 6.4 Sv) of Atlantic Water enteres the Arctic Ocean through the Fram Strait and most goes into the shallow Barents Sea. With Neptune parameterization in run B, this discrepancy is improved to some extent, with 43% (2.7 of 6.3 Sv) of Atlantic Water entering through the Fram Strait. Run C produces the most accurate distribution of the three runs with two thirds (3.9 of 5.8 Sv) of Atlantic Water entering the Arctic Ocean through the Fram Strait. However, this is still less than observational results that show ca. 85% of Atlantic Water entering the Arctic Ocean through the Fram Strait.

Absolute values of inflow at the FS are underestimated in all three model runs. Run A produces an inflow of only 1.8 Sv at the FS. The inflow at the FS increases by 50% to 2.7 Sv after adopting Neptune parameterization in run B. The high-resolution model run C generates the best result, but the volume transport of 3.9 Sv at the FS is still much smaller than observed values of 9–12 Sv. All three model runs in this study therefore underestimate the volume transport at the FS, and Wang et al.[21] also reported similar findings for several different model results. The results of their study also showed that the accuracy of both simulated inflow and outflow were related to horizontal resolution[21].

For the BSO, both ORCA1-grid runs (A and B) overestimate inflow volume transport. Run C reproduces a realistic

inflow transport and the velocity field is clearly shown with two cores in the northern and southern parts of the opening (not shown), similar to the results of Aksenov et al.[11].

Heat transport is estimated by integrating temperature multiplied by volume transport for each cell. The distribution of heat transport is also misrepresented by the three model runs. The output from run A shows that most of the heat is advected to the Arctic Ocean through the BSO rather than the FS, resulting in an unrealistically low heat input to the Eurasian Basin. Run B is better than run A but run C generates the best results with a reasonable distribution compared with observational data.

The heat transport at the FS in run A is 21 TW, roughly half of the observed value. Using Neptune parameterization in run B almost doubles the heat transport at the FS (39 TW, Table 2). The improvement of only 50% in volume transport implies that the temperature field at the FS is also improved (contour lines in Figure 5). Moreover, the WSC is better reproduced with Neptune parameterization, so more warm Atlantic Water from the sub-polar GIN seas can reach the FS, resulting in higher temperatures (not shown, similar results are presented in Wang et al.[21], Figure 3). The ratios of heat and volume transport from run A and run C are similar; run C generated values ~2.2 times larger for both volume and heat transport.

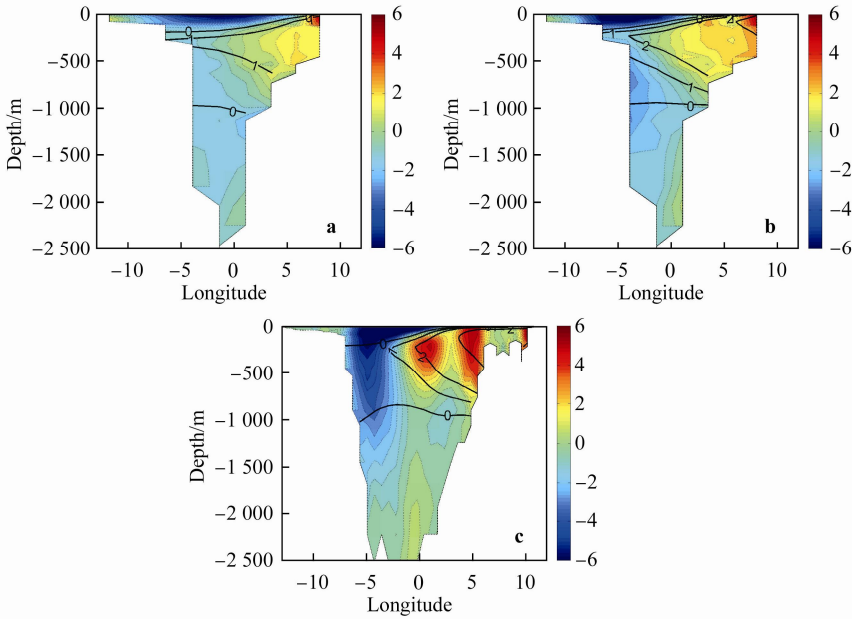

Figure 5 Annual mean normal velocity through the Fram Strait (cm·s^{-1}, shading) and temperature (contour line). Positive values indicate the northward flow, negative values indicate the southward flow. Solid lines indicate temperatures from 0–3℃ at 1℃ intervals.

At the BSO, although the inflow of heat is very large, the heat is almost completely lost in the Barents Sea[12]. When the BSB reaches the eastern Eurasian Basin at the St. Anna Trough, the temperature of the AWCT is only a little higher than 0℃. This branch has no influence on the AWCT in the western part of the Eurasian Basin that we focus on in this study. However, the excess inflow of the BSB may affect the circulation and thermohaline structure in the eastern part of the basin. That will be discussed briefly in the last section of this paper.

6 Details of velocity at the Fram Strait

The velocity patterns in the Fram Strait are similar in run A and run B (Figure 5a and 5b) but improvements are obtained in run B at both the eastern and western sides of the Strait. The inflow of the WSC is improved although underestimated, and only one core can be resolved. The Yermak Plateau Branch (YPB) (Figure 1) is obvious in run B (Figure 3b and Figure 4b), and is similar to that reproduced by Holloway and Wang's[20] simulation using a coarse grid and Neptune parameterization. And also to the west, the EGC is recognizable at the intermediate depth. Run C reproduces a stronger velocity field with a maximum of about 6 cm·s^{-1} at the eastern part of the Fram Strait, compared with 4–5 cm·s^{-1} for the runs using a coarse grid.

Run C (Figure 5c) reveals almost all currents identified using observational data or previous model results[32,11]. The West Spitsbergen Coastal Current (WSCC) inflow is seen over the shallow shelf. The Svalbard Branch (SVB) and the Yermak Plateau Branch (YPB) are difficult to distinguish in the velocity field section, but are obvious in Figures 3c and 4c. These two branches were also identified by the high-resolution models used by Aksenov et al.[11]. The simulated velocity for the SVB of ~6 cm·s^{-1} is still slower than the observed value of 10–20 cm·s^{-1}[32] and model results of 14 cm·s^{-1} reported by Aksenov et al.[11]. The velocity of re-circulation in the Knipovich Branch (KB) is about 5 cm·s^{-1}, which is also slower than velocity measured from observations[31], but faster than that generated

using models in Aksenov et al.[11], which produced a velocity of ~2 cm·s^{-1}. The southward KB is not well resolved in the annual mean velocity field, and Aksenov et al.[11] also failed to reproduce it accurately, but this current can be identified from monthly output (not shown). The YPB and the KB are apparently guided by the Yermak Plateau and the Knipovich Ridge. The eddy-topography interaction may therefore dominate these flows and Neptune parameterization can effectively supply this effect for a coarse resolution model.

Many observations have demonstrated that velocity through the FS section is very complex and belt-like. The ORCA1 grid has only 10 points at the Fram Strait, therefore the low resolution of ORCA1 in this area may be the main cause for the failure of models to reproduce this complex velocity field. Run C, using the ORCA025 grid with a higher horizontal resolution, successfully resolves several cores representing split branches of the WSC but the velocity of the inflow is still underestimated compared with observational results and model results presented by Aksenov et al.[11] who used a 1/12 degree horizontal resolution. At the Fram Strait, the Rossby Deformation Radius is less than 10 km so the ORCA025 grid is eddy-permitting but not eddy-resolving. A more realistic velocity field can be reasonably reproduced by an eddy-resolving model as used by Aksenov et al.[11].

7 Discussion and conclusions

In this paper, we present the results of AIW simulations in the Eurasian Basin generated from three model runs. The baseline run (run A) drifts from PHC data with about half of the heat content being lost in station A. Using Neptune parameterization (run B) and a high-resolution horizontal grid (run C) helps to improve the representation of AIW in the numerical models, including the AWCT and its depth. The values for volume and heat transport through the Fram Strait generated by run B are closer to observational results than those for run A, but run C is the best among the three runs. The high-resolution model allows for more Atlantic Water entering the Arctic Basin. Furthermore, run C produces the best distribution of volume transport between the FS and the BSO, although the inflow through the Fram Strait is still less than observational values. We suggest that the reason the baseline run failed to reproduce the AIW is the underestimation of the modeled WSC, leading to a lack of heat transport through the Fram Strait.

In the coarse (ORCA1) grid model, Neptune parameterization improves the simulation of the circulation of the ACBC and the water properties at intermediate depth in the western Eurasian Basin. This parameterization can significantly improve representation of the ACBC in a non-eddy-permitting model. Neptune parameterization is applied directly into momentum equations, in an attempt to maintain currents flowing along the topographic Rossby waves, which are not directly reflected in the tracer equations. Hence, the density structure might not be adapted appropriately, and this needs further investigation. In this study, Neptune parameterization proves to be an effective tool for improving topographic flows in non-eddy-permitting models.

The performance of models in simulating topography-steered flow is affected by the horizontal resolution in several ways, including the interaction between eddies and topography. The results of this study suggest that eddy-permitting models are necessary to obtain a realistic representation of circulation in the Arctic Ocean and the Nordic Sea. The Rossby Deformation Radius is small in polar regions, therefore the model resolution should be less than several kilometers to accurately reproduce complex velocity fields with more than one core. The complexity of the velocity field at the FS has been confirmed by Schauer et al.[32] using mooring data. The findings of their study suggested a barotropic structure with many inflow and outflow belts varying in size by several tens of kilometers[33]. In run C, the microstructure of the ACBC is well represented with two velocity cores identified to the north of Franz-Josef Land (not shown). One of these cores was the FSB from the FS and the other is the higher velocity Arctic Shelf Break Branch (ASBB[14]) close to the shelf. In run A and run B, only one velocity core is resolved, which results in an underestimation of the water masses carried by the ACBC. Neptune parameterization has also been effective in fine resolution models, especially for eddy-permitting models (personal communication with Holloway). Investigation of the performance of Neptune parameterization in fine resolution models, and impacts on the AIW, are beyond the scope of this paper but should be addressed in future work.

The AWCT is slightly higher in the western part of the Eurasian Basin (Figure 2) but it decreases abruptly by ~1℃ within about 200 km (not shown), just north of the St. Anna Trough. Our assumption is that the BSB inflow through the St. Anna Trough is overestimated. However, the problem in the eastern part of the Eurasian Basin may be a complicated issue with many contributing factors, including excessive vertical diffusion as discussed by Li et al.[26], the congregation of horizontal ORCA grids in this area, and too much mixing with the BSB from the St. Anna Trough. More research is needed to improve model simulations of the eastern part of the Eurasian Basin, north of the Laptev Sea.

Acknowledgements This study was supported by the "Plan 111" (Grant no. B07036), the National Natural Science Foundation of China (NNSFC) (Grant no. 40631006), and the International Cooperate Fund of NNSFC (Grant no. 40810104046). We thank Dr. Greg Holloway for introducing the Neptune effect. We also appreciate the help received from Dr. Frederic Dupont and Mr. Biao Shen with problems of model restart and debugging.

References

1 Pachauri R K, Reisinger A, et al. Climate Change 2007: Synthesis Report, Contribution of Working Groups I, II and III to the Fourth Assessment Report of the Intergovernmental Panel on Climate Change. IPCC, 2007, ISBN92-9169-122-4.

2 Serreze M C, Holland M M, Stroeve J. Perspectives on the Arctic's shrinking sea ice cover. Science, 2007, 315(5818): 1533–1536, doi:10.1126/science.1139426.

3 Steele M, Boyd T. Retreat of the cold halocline layer in the Arctic Ocean. J Geophys Res, 1998, 103(C5): 10419–10435, doi:10.1029/98JC00580.

4 Boyd T J, Steele M, Muench R, et al. Partial recovery of the Arctic Ocean halocline. Geophys Res Lett, 2002, 29(14): 2-1–2-4, doi: 10. 1029/2001GL014047.

5 Polyakov I V, Alekseev G V, Timokhov L A, et al. Variability of the intermediate atlantic water of the arctic ocean over the Last 100 Years. J Climate, 2004, 17(23): 4485–4497.

6 Rudels B, Anderson L G, Jones E P. Formation and evolution of the surface mixed layer and halocline of the Arctic Ocean. J Geophys Res, 1996, 101(C1): 8807–8821.

7 Polyakov I V, Beszczynska A, Carmack E, et al. One more step toward a warmer Arctic. Geophys Res Lett, 2005, 32(17): L17605, doi:10.1029/2005GL023740.

8 Polyakov I V, Alexeev V V, Ashik I M, et al. Fate of Early-2000s arctic warm water pulse. Bull Amer Meteor Soc, 2011, 92(5): 561–566, doi:10.1175/2010BAMS2921.1.

9 Rudels B, Jones E P, Anderson L G, et al. On the intermediate depth waters of the Arctic Ocean. Geophys Monogr Ser, 1994, 85: 33–46.

10 Rudels B, Friedrich H J, Quadfasel D. The Arctic circumpolar boundary current. Deep Sea Res Part II, 1999, 46(6-7): 1023–1062.

11 Aksenov Y, Bacon S, Coward A C, et al. The North atlantic inflow to the arctic Ocean: High resolution model study. J Mar Syst, 2010, 79(1-2): 1–22, doi:10.1016/j.jmarsys.2009.05.003.

12 Wang J, Jin M B, Takahashi J, et al. Modeling arctic ocean heat transport and warming episodes in the 20th century caused by the intruding Atlantic Water. Chinese J Polar Sci, 2008, 19(2): 159–167.

13 Aksenov Y, Ivanov V V, Nurser A J G, et al. The Arctic circumpolar boundary current. J Geophys Res, 2011, 116(C9), C09017, doi:10.1029/2010JC006637.

14 Proshutinsky A, Steele M, Zhang J, et al. Multinational effort studies differences among Arctic Ocean models. EOS, AGU, 2001, 82(51): 637–644, doi:10.1029/01EO00365.

15 Holloway G, Dupont F, Golubeva E, et al. Water properties and circulation in Arctic Ocean models. J Geophys Res, 2007, 112(C4), C04S03, doi:10.1029/2006JC003642.

16 Yang J Y. The Arctic and subarctic Ocean flux of potential vorticity and the Arctic Ocean circulation. J Phys Oceanogr, 2005, 35(12): 2387–2407.

17 Holloway G. A shelf wave/topographic pump drives mean coastal circulation. Ocean Modelling, 1986, 68: 12–15.

18 Golubeva E N, Platov G A. On improving the simulation of Atlantic Water circulation in the Arctic Ocean. J Geophys Res, 2007, 112(C4), C04S05, doi:10.1029/2006JC003734.

19 Polyakov I V. An eddy parameterization based on maximum entropy production with application to modeling of the Arctic Ocean circulation. J Phys Oceanogr, 2001, 31(8): 2255–2270.

20 Holloway G, Wang Z. Representing eddy stress in an Arctic Ocean model. J Geophys Res, 2009, 114(C6), C06020, doi:10.1029/2008JC005169.

21 Wang Z L, Holloway G, Hannah C. Effects of parameterized eddy stress on volume, heat, and freshwater transports through Fram Strait. J Geophys Res, 2011, 116(C8), C00d09, doi:10.1029/2010JC006871.

22 Holloway G, Nguyen A, Wang Z L. Oceans and ocean models as seen by current meters. J Geophys Res, 2011, 116(C8), C00D08, doi:10.1029/2011JC007044.

23 Madec G. NEMO ocean engine. Note du Pole de modélisation, Institut Pierre-Simon Laplace (IPSL), 2008, France, No 27, ISSN No. 1288–1619.

24 Madec G, Delecluse P, Imbard M, et al. OPA 8. 1 Ocean General Circulation Model reference manual. Note du Pole de modélisation, Institut Pierre-Simon Laplace (IPSL), 1998, 11: 91.

25 Fichefet T, Morales Maqueda M A. Sensitivity of a global sea ice model to the treatment of ice thermodynamics and dynamics. J Geophys Res, 1997, 102(C6): 12609–12646, doi:10.1029/97JC00480.

26 Li X, Su J, Zhang Y, et al. Discussion on the simulation of Arctic intermediate water under NEMO framework // Proceedings of Twentieth (2011) International Offshore and Polar Engineering Conference, Hawaii, 2011, 1: 953–957.

27 Steele M, Morley R, Ermold W. PHC: A global ocean hydrography with a high quality Arctic Ocean. J Climate, 2001, 14(9): 2079–2087.

28 Gent P R, McWilliams J C. Isopycnal mixing in ocean circulation models. J Phys Oceanogr, 1990, 20(1): 150–155.

29 Hunke E, Maltrud M, Holland M, et al. GM vs biharmonic ocean mixing in the Arctic. J Phys: Conf Ser, 2005, 16: 348–352, doi:10.1088/1742-6596/16/1/048.

30 Merryfield W, Scott R. Bathymetric influence on mean currents in two high-resolution near-global ocean models. Ocean Modelling, 2007, 16(1-2): 76–94.

31 Holloway G. Observing global ocean topostrophy. J Geophys Res, 2008, 113(C7), C07054, doi:10.1029/2007JC004635.

32 Schauer U, Fahrbach E, Osterhus S, et al. Arctic warming through the Fram Strait: Oceanic heat transport from 3 years of measurements. J Geophys Res, 2004, 109(C6), C06026, doi:10.1029/2003JC001823.

33 Skagseth Ø, Furevik T, Ingvaldsen R B, et al. Volume and heat transports to the Arctic Ocean via the Norwegian and Barents seas // Dickson R R, Meincke J, Rhines P. Arctic-Subarctic Ocean Fluxes: Defining the Role of the Northern Seas in Climate. In Arctic-Subarctic Ocean Fluxes, Dordrecht, Netherlands: Springer, 2008: 45–64.

34 Schauer U, Beszczynska-Moller A, Walczowski W, et al. Variation of measured heat flow through the Fram Strait between 1997and 2006 // Dickson R R, Meincke J, Rhines P. In Arctic-Subarctic Ocean Fluxes. Dordrecht, Netherlands: Springer, 2008: 65–85.

35 Smedsrud L H, Ingvaldsen R, Nilsen J E, et al. Heat in the Barents Sea: Transport, storage, and surface fluxes. Ocean Science, 2010, 6(1): 219–234, doi:10.5194/ os-6–219-2010.